POLITECNICO DI TORINO
Repository ISTITUZIONALE

Geometrical Descriptors for Human Face Morphological Analysis and Recognition

(Article begins on next page)

04 August 2020

Geometrical Descriptors for Human Face Morphological Analysis and Recognition

Enrico Vezzetti, Federica Marcolin
Dipartimento di Sistemi di Produzione ed Economia dell'Azienda
Politecnico di Torino

Abstract

The human eye, connected to the brain, gives people the possibility to immediately, automatically and exactly recognize one person from another. A main aim is obviously to "copy" this recognition mechanism of the brain and to use it as a means for face recognition. Since the human recognition happens through an automatic "authentication" of facial shape and features, this face study is totally Geometry-based. In order to formalize the anatomical facial features, many strategies may be used. This work collects various solutions.

Particularly, a geometrical description of human face is here proposed as a survey. Some elements of Differential Geometry, such as the Coefficients of the Fundamental Forms, the Principal Curvatures, Mean and Gaussian Curvatures, the derivatives and the Shape and Curvedness Indexes introduced by Koenderink and VanDoorn are briefly defined and explained, and then used as descriptors for three-dimensional facial surface. Their behaviour on faces is classified according to some feedback parameters: similarity between different faces, sensitivity to noise, completeness and smoothness.

Face is the most important part of human anatomy, and its study has many scopes. This survey may be used as a starting point for elaborating and implementing an algorithm for 3D facial recognition.

1. Introduction

Face recognition is a task involving our lifes daily. The nowadays attempt is to automate it in computers through targeted algorithms, in order to use it as a means suitable for the study and able to perform both authentication and recognition. The purposes are various, but belong to three big branches: face verification, or *authentication*, to guarantee secure access; face *identification*, or recognition of suspects, dangerous individuals and public enemies by Police, FBI and other safety organizations; and maxillofacial *surgery*, for studying the faces which surgeons have to deal with. As can be imagined, automatization is necessary. In particular, a facial recognition system is a computer application for automatically identifying or verifying a person from a digital image or a video frame from a video source. Some popular recognition algorithms are Principal Component Analysis, used by Lei *et al.* [23], Mian [25] and Xue *et al.* [56], Hidden Markov Models, used by Yi *et al.* [37], and Iterative Closest Point, used by Amor *et al.* [3], Amberg *et al.* [2], Alyuz *et al.* [1], Xiaoguang *et al.* [36], Yong-An *et al.* [38] and Smeets *et al.* [30].

Although 2D facial recognition was introduced earlier and was the first to be automated, in the late 1980s the advantages of 3D recognition emerged. Three-dimensional face recognition is a method for facial recognition in which the three-dimensional geometry of the human face is used. It has been shown that 3D face recognition methods can achieve significantly higher accuracy than their 2D counterparts, rivaling fingerprint recognition. 3D face recognition has the potential to achieve better accuracy than its two-dimensional counterpart by measuring geometry of rigid features on the face. This avoids such pitfalls of 2D face recognition algorithms as change in lighting, different facial expressions, make-up and head orientation. The main novelty of this approach is the ability to compare surfaces independent of natural deformations resulting from facial expressions. First, the range image and the texture of the face are acquired. Next, the range image is preprocessed by removing certain parts such as hair, which can complicate the recognition process. Finally, a canonical form of the facial surface is computed. Such a representation is insensitive to head

orientations and facial expressions, thus significantly simplifying the recognition procedure. The recognition itself is performed on the canonical surfaces [41].

The method emerged significantly later than the other ones because of the technological limitation of acquisition of three-dimensional images. However, nowadays it can easily be possible to obtain 3D shootings just through the use of two or more 2D cameras pointing to the same subject: intersecting the views a 3D image is obtained. It's the method used to realize the three-dimensional effects of the latest movies. Since many public areas are shot by more cameras, a 3D recognition is possible.

Starting from this concept, Elyan *et al.* [11] presented a technique for 3D face recognition system using a set of parameters representing the central region of the face. These parameters are essentially vertical and cross sectional profiles and are extracted automatically without any prior knowledge or assumption about the image pose or orientation. In addition, these profiles are stored in terms of their Fourier Coefficients in order to minimize the size of input data. Cadavid *et al.* [4] presented a method for 3D face recognition using adaboosted geodesic distance features. AdaBoost generates a strong-classifier based on a collection of geodesic distances that are most discriminative for face recognition. Fabry *et al.* [13] presented a general 3D face recognition method based on point cloud kernel correlation and kernel density estimation for registration, which doesn't make use of a training set of faces or point correspondences and can handle noisy, unpreprocessed face scans. Queirolo *et al.* [27] [28] combined a Simulated Annealing-based approach (SA) for image registration using the Surface Interpenetration Measure (SIM) to perform a precise matching between two face images. Harguess *et al.* [20] presented an analysis on using the pattern of symmetry in the face to increase the accuracy of three-dimensional face recognition. They introduced the concept of the "dasia average-half-face psila", motivated by the symmetry preserving singular value decomposition. Gunlu *et al.* [18] [19] presented a method for 3D facial feature extraction. In this method, 3D discrete cosine transform (DCT) is used to extract features. The coefficients of 3D transformation are calculated and the most discriminant 3D transform coefficients are selected as feature vector where the ratio of within-class variance and between-class variance is used as selection measure. They also investigate the proposed approach by using 3D discrete Fourier transform instead of 3D DCT for comparison.

Anyway, if all these works show how recognition is possible with the use of different algorithms, mathematical operators, models and descriptors, no ones deal with the geometrical description of anatomical facial features. The brain gives human beings the possibility to recognize immediately persons, as an automatic process. Since the brain is unfailing, the possibility to computationally elaborate the same recognizing procedure gives the research a strong method for the face recognition. Excluding the typical colours of a person, namely skin, eyes and hair, the shape of the components of the faces are clearly the most important elements to establish a correspondence between a face and another. That is why a deep geometrical study of facial surface is so important. The use of some main notions and formalisms of Differential Geometry is necessary. This is exactly the starting point of the study.

2. Geometrical Descriptors

Some main notions of geometry are used to study the facial surface behaviour and help recognition. After introducing the definition of free-form surface, a summary of differential geometry basic coefficients and curvatures is here presented. Furthermore, shape and curvedness indexes are explained. All the elements explained in this section will be used as descriptors in the next one.

Classical differential geometry is the study of local properties of curves and surfaces. A patch or local surface is a differentiable mapping $x: U \rightarrow \Re^n$, where U is an open subset of $\Re^2$. Actually, a facial surface is not a well-known patch: it is a free-form surface. A *free-form surface* is defined to be a smooth surface, such that the surface normal is well defined and continuous almost everywhere, except at vertices, edges, and cusps [8]. They talk about free-form surfaces of

sculptures, car bodies, human bodies and faces, airplanes, boat hulls and soil trends: they are piecewisesmooth. Free-form is a characterization of an object whose surfaces do not belong to classes easily categorizable as flat surfaces or quadrics. Accordingly, it is assumed that a free-form object consists of one or more "non-flat and non-quadric" surfaces. Alternatively, a free-form surface is rigorously defined as "a manifold of unknown equation which, thanks to suitable assumptions of regularity in the main function, the directional derivative calculated at any point, on the overall profile of partial curvatures, can be decomposed into subdomains through an artifice. Each subdomain, in turn, can be studied as a combination of simple geometries such as spherical shells, cones, cylinders, paraboloids and saddles". In the next part of the paper the human face is treated as a free-form object characterized by sufficient regularity and composed by easily identifiable surfaces. The operators and curvatures used below can be applied to patches and free-form surfaces in the same way.

Since a patch can be written as an *n*-tuple of functions

$$x(u,v) = \left(x_1(u,v),...,x_n(u,v)\right),$$

the partial derivative of *x* with respect to *u* can be defined by

$$x_u = \left(\frac{\partial x_1}{\partial u},...,\frac{\partial x_n}{\partial u}\right).$$

The other partial derivatives are defined similarly.

2.1 Coefficients of the Fundamental Forms

It is possible to measure distances on a surface. In Euclidean space $\Re^n$, if $\underline{p} = \left(p_1,...,p_n\right)$ and $\underline{q} = \left(q_1,...,q_n\right)$ are points in $\Re^n$, then the distance *s* from $\underline{p}$ to $\underline{q}$ is given by

$$s^2 = \left(p_1 - q_1\right)^2 + ... + \left(p_n - q_n\right)^2.$$

Because a general surface is curved, distance on it is not the same as in Euclidean space; in particular, the form above is in general false however the coordinates are interpreted. To describe how to measure distance on a surface, the mathematically imprecise concept of an "infinitesimal" is necessary. The infinitesimal version of that for $n = 2$ for a surface is

$$ds^2 = Edu^2 + 2Fdudv + Gdv^2,$$

called First Fundamental Form, or Riemann Metric. This is the classical notation for a metric on a surface. *E*, *F*, *G* are functions $U \rightarrow \Re$ such that:

$$E = \|x_u\|^2,$$

$$F = \langle x_u, x_v \rangle,$$

$$G = \|x_v\|^2,$$

and are called *Coefficients of the First Fundamental Form*. These coefficients are given by inner products of the partial derivatives of the surface. Therefore, the First Fundamental Form is merely the expression of how the surface inherits the natural inner product of $\Re^3$. Geometrically, the first fundamental form allows to make measurements on the surface (lengths of curves, angles of tangent vectors, areas of regions) without referring back to the ambient space $\Re^3$ where the surface lies [7].

To introduce the Second Fundamental Form, the definitions of Gauss map must be given. For an injective patch *x: U → $\Re^n$* the unit normal vector field or surface normal N is defined by

$$N(u,v) = \frac{x_u \times x_v}{|x_u \times x_v|}(u,v)$$

at those points $(u,v) \in U$ at which $x_u \times x_v$ does not vanish [17]. The map that assigns to each point p on a surface the point on the unit sphere $S^2(1) \subset \Re^3$ that is parallel to the unit normal $N(p)$, or N_p, is called the Gauss Map.

Let $x: U \to \Re^n$ be a regular patch. Then

$$e = -\langle N_u, x_u \rangle = \langle N, x_{uu} \rangle,$$

$$f = -\langle N_v, x_u \rangle = \langle N, x_{uv} \rangle = \langle N, x_{vu} \rangle = -\langle N_u, x_v \rangle,$$

$$g = -\langle N_v, x_v \rangle = \langle N, x_{vv} \rangle$$

are called the *Coefficients of the Second Fundamental Form* of x, and $edu^2 + 2fdudv + gdv^2$ is the Second Fundamental Form of the patch x.

Very often a surface is given as the graph of a differentiable function $z = h(x, y)$, where (x, y) belong to an open set $U \to \Re^2$. It is, therefore, convenient to have at hand formulas for the relevant concepts in this case. To obtain such formulas let us parametrize the surface by

$$x(u, v) = (u, v, h(u, v)), \qquad (u, v) \in U,$$

where $u = x$, $v = y$. A simple computation shows that

$$x_u = (1, 0, h_u),$$

$$x_v = (0, 1, h_v),$$

$$x_{uu} = (0, 0, h_{uu}),$$

$$x_{uv} = (0, 0, h_{uv}),$$

$$x_{vv} = (0, 0, h_{vv}).$$

Thus

$$N(x, y) = \frac{(-h_x, -h_y, 1)}{\sqrt{1 + h_x^2 + h_y^2}}$$

is a unit normal field on the surface, and the Coefficients of the Second Fundamental Form in this orientation are given by

$$e = \frac{-h_{xx}}{\sqrt{1 + h_x^2 + h_y^2}},$$

$$f = \frac{-h_{xy}}{\sqrt{1 + h_x^2 + h_y^2}}, \qquad (1)$$

$$g = \frac{-h_{yy}}{\sqrt{1 + h_x^2 + h_y^2}}.$$

From the above expressions, any needed formula can be easily computed. For instance, the Coefficients of the First Fundamental Form are obtained:

$$E = 1 + h_x^2,$$

$$F = h_x h_y, \qquad (2)$$

$$G = 1 + h_y^2.$$

Some authors used Fundamental Forms for recognition, images processing and motion analysis. Elad *et al.* [9] presented a method to construct a bending invariant canonical form for such surfaces. This invariant representation is an embedding of the intrinsic geodesic structure of the surface in a finite dimensional Euclidean space, in which geodesic distances are approximated by Euclidean ones. The canonical representation is constructed by first measuring the intergeodesic distances between points on the surfaces. Next, multi-dimensional scaling (MDS) techniques are applied to extract a finite dimensional flat space in which geodesic distances are represented as Euclidean ones. The geodesic distances are measured by the efficient fast marching on triangulated domains numerical algorithm. Applying this transform to various objects with similar geodesic

structures (similar First Fundamental Form) maps isometric objects into similar canonical forms. Isometric surfaces share the same geometric structure, also known as the First Fundamental Form. Then, they presented a method to construct a bending invariant signature for such surfaces [10]. In his various publications Goldgof *et al.* [14] [15] [16] presented a new algorithm for recovering motion parameters of non-rigid objects using both point and line correspondences between 3D surfaces. It requires estimating the coefficients of the first fundamental form before and after the motion. A vector point function is utilized as the motion parameter, called the "displacement function". Differential-geometric changes of surfaces are then used in tracking small deformations. Discriminant of First Fundamental Form, unit-normal and Gaussian Curvature are the invariant differential-geometric parameters that have been utilized for non-rigid motion analysis.

2.2 Curvatures

Curvatures are used to measure how a regular surface x bends in $\Re^3$. One way to do this is to estimate how the tangent plane changes from point to point.

The two-dimensional vector subspace $Dx(q) \subset \Re^3$, where D is the differential and q is a point of U, coincides with the set of tangent vectors to x at $x(q)$ [7]. By the above proposition, the plane $Dx(q)$, which passes through $x(q) = p$, does not depend on the parametrization. This plane will be called the tangent plane to x at p and will be denoted by $T_p(x)$. For each p there exists an orthonormal basis $\{e_1, e_2\}$ of $T_p(x)$ such that $DN_p(e_1) = -k_1 e_1$, $DN_p(e_2) = -k_2 e_2$. Moreover, k_1 and k_2 ($k_1 \geq k_2$) are the maximum and minimum of the Second Fundamental Form restricted to the unit circle of $T_p(x)$. The maximum curvature k_1 and the minimum curvature k_2 introduced above are called the *Principal Curvatures* at p; the corresponding directions, that is, the directions given by the eigenvectors e_1, e_2 are called Principal Directions at p [7]. For instance, in the plane all directions at all points are principal directions. The same happens with a sphere. In both cases, this comes from the fact that the second fundamental form at each point is constant.

The determinant of DN is the product $(-k_1)(-k_2) = k_1 k_2$ of the Principal Curvatures, and the trace of DN is the negative $-(k_1 + k_2)$ of the sum of Principal Curvatures. If the orientation of the surface is changed, the determinant does not change (the fact that the dimension is even is essential here); the trace, however, changes sign. Particularly, in point p, the determinant of DN_p is the *Gaussian Curvature K* of x at p. The negative of half of the trace of DN is called the *Mean Curvature H* of x at p [7].

In terms of the principal curvatures can be written

$K = k_1 k_2$,

$H = \dfrac{k_1 + k_2}{2}$.

At an elliptic point the Gaussian curvature is positive. Both principal curvatures have the same sign, and therefore all curves passing through this point have their normal vectors pointing toward the same side of the tangent plane. The points of a sphere are elliptic points. At a hyperbolic point, the Gaussian curvature is negative. The principal curvatures have opposite signs, and therefore there are curves through p whose normal vectors at p point toward any of the sides of the tangent plane at p. At a parabolic point, the Gaussian Curvature is zero, but one of the principal curvatures is not zero. The points of a cylinder are parabolic points. Finally, at a planar point, all principal curvatures are zero. The points of a plane trivially satisfy this condition.

The Gaussian curvature and the mean curvature of x are given by the formulas

$$K = \frac{eg - f^2}{EG - F^2},$$

$$H = \frac{eG - 2fF + gE}{2(EG - F^2)},$$

where *E, F, G, e, f, g* are the Coefficients of the Fundamental Forms. Using the parametrization such that $z = h(x, y)$, an alternative form for *K* and *H* are obtained:

$$K = \frac{h_{xx}h_{yy} - h_{xy}^2}{\left(1 + h_x^2 + h_y^2\right)^2},$$

$$H = \frac{\left(1 + h_x^2\right)h_{yy} - 2h_x h_y h_{xy} + \left(1 + h_y^2\right)h_{xx}}{\left(1 + h_x^2 + h_y^2\right)^{3/2}}.$$

(3)

The forms with *h* were implemented in the numerical computation and used to generate the facial images presented later.

The Principal Curvatures are the roots of the quadratic equation

$$x^2 - 2Hx + K = 0.$$

Thus k_1 and k_2 can be chosen so that

$$k_1 = H + \sqrt{H^2 - K},$$

$$k_2 = H - \sqrt{H^2 - K}.$$

(4)

Some researchers used curvature as a means for recognition. Mahoor *et al.* [24] presented an approach for 3D face recognition from range data based on the principal curvature, k_{max}, and Hausdorff distance. They use the principal curvature to represent the face image as a 3D binary image called ridge image, which shows the locations of the ridge lines around the important facial regions on the face. D'Hose *et al.* [6] presented a method for localization of particular features on 3D faces using Gabor wavelets to extract the curvature of the 3D faces, which is then used for performing a coarse detection of landmarks. Sun *et al.* [32] proposed to use a generic model to label the 3D facial features. This approach relies on their realistic face modelling technique, by which the individual face model is created using a generic model and two views of a face. In the individualized model, they label the face features by their maximum and minimum curvatures. Ming *et al.* [26] proposed a framework for 3D face recognition based on depth information, whose core is Orthogonal Laplacianfaces (OLPP), a method for utilizing a Euclid space into which data points are mapped and for producing orthogonal basis functions. In order to overcome facial expression variation, they first utilize curvature information projected onto the moving least-squares (MLS) surface to segment a face rigid area, which is insensitive to expression variation. In a survey of the available methodologies and parameters for reverse engineering, Vezzetti *et al.* [34] identified the Gaussian Curvature as a possible morphological descriptor, employing it in the methods of Percentiles, Angle Deficit and Quadratic Surface Fitting.

2.3 Derivatives

The derivatives with respect to the horizontal and vertical coordinates are an important descriptor for facial surface behaviour, although their information is contained in other geometrical elements, such as the curvatures and the coefficients of the Fundamental Forms. Anyway they are used here as a separate parameter, because the other descriptors do not carry all the information the derivatives themselves do. The *derivative* is a measure of how a function changes as its input changes. Formally, the first derivative of the one-variable function *f* at *a* is the limit

$$f'(a) = \lim_{h \to o} \frac{f(a + h) - f(a)}{h}$$

of the different quotient as *h* approaches to zero, if the limit exists. The second derivative f'' is the derivative of the first derivative, if it exists. As its definition explains, the first derivative describes the slope of the facial surface and, consequently, identify the critical points, namely the points in which the derivative is equal to zero; while the second derivative tells us if those critical points are maximums, minimums or inflections. If $f''(a) < 0$, then *a* is a local maximum of the function *f*; if $f''(a) > 0$, then *a* is a local minimum; while, if $f''(a) = 0$, then *a* is an inflection point. The discussion can be extended to other dimensions, namely to functions with more variables, using the Hessian Matrix instead of the second derivative. The first derivatives with respect to x and y, the second and mixed derivatives are here used as descriptors.

Derivatives are widely used in many ways for face recognition purposes. Yongsheng et al. [39] proposed a novel high-order local pattern descriptor, local derivative pattern (LDP), for face recognition. LDP is a general framework to encode directional pattern features based on local derivative variations. The *nth*-order LDP is proposed to encode the (*n*-1)*th* -order local derivative direction variations, which can capture more detailed information than the first-order local pattern used in local binary pattern (LBP). Then proposed a new Circular Derivative Pattern (CDP) which extracts high-order derivative information of images along circular directions. They argue that the high-order circular derivatives contain more detailed and more discriminative information than the first-order LBP in terms of recognition accuracy [40]. Jinye *at al.* [21] analyzed theoretically the derivative feature of ASBW by which the gradient vector of a facial image at every resolution level can be obtained. Then an analysis of the robustness of directional gradient angles of facial images is presented. Then we propose a multi-scale Bayesian face recognition based on ASBW. Essannouni *et al.*'s main objective [12] was to automate face tracking and verify the identity of the person. In fact the most pure algorithms of tracking has two major problems, namely the initialization problem and the lost track problem. To avoid these problems, the initialization is done by real time face detector. The verification of the presence of the searched face is done using a new technique of template matching based on robust correlation of the orientation of the second derivatives. The tracking is done using the Sum of Squared Difference (SSD).

2.4 Shape and Curvedness Indexes

Several techniques have been developed to estimate the curvature information in the last two decades. From the mathematical viewpoint, the curvature information can be retrieved by the first and second partial derivatives of the local surface, the local surface normal and the tensor voting [33]. An interesting curvature representation was proposed by Koenderink *et al.* [22]. It is based on the parametrization of the structure in two features maps, namely the Shape Index *S* and the Curvedness Index *C*. The formal definition of *Shape Index* can be given as follows:

$$S = -\frac{2}{\pi} \arctan \frac{k_1 + k_2}{k_1 - k_2}, \qquad S \in [-1,1], \qquad k_1 \geq k_2. \qquad (5)$$

It describes the shape of the surface. Koenderink *et al.* proposed a partition of the range [-1,1] in nine categories, which correspond to nine different surfaces. In this paper a simplified scale is used, with seven categories, proposed by Vezzetti *et al.* [33] and Calignano [5].

This representation has many intuitively "natural" properties [22]:

- two shapes for which the Shape Index differs merely by sign represent complementary pairs that will fit together as "stamp" and "mould" when suitably scaled;
- the shape for which the Shape Index vanishes - and consequently has indeterminate sign - represents the objects which are congruent to their own moulds;
- convexities and concavities find their places on opposite sides of the shape scale. These basic shapes are separated by those shapes which are neither convex nor concave, that are the saddlelike objects. The transitional shapes that divide the convexities/concavities from the saddle-shapes are the cylindrical ridge and the cylindrical rut;

- if shapes are drawn at random from an isotropic distribution in the (k_1, k_2)-plane, then the Shape Index scale will be uniformly covered, thus the scale is "well tempered". This follows immediately from the fact that the Shape Index S is directly proportional to the angle with the $k_1 + k_2 = 0$-axis.

S does not give an indication of the scale of curvature present in the shapes. For this reason, an additional feature is introduced, the *Curvedness Index* of a surface:

$$C = \sqrt{\frac{k_1^2 + k_2^2}{2}}. \qquad (6)$$

It is a measure of how highly or gently curved a point is and is defined as the distance from the origin in the (k_1, k_2)-plane. Whereas the Shape Index scale is quite independent of the choice of a unit of length, the curvedness scale is not. Curvedness has the dimension of reciprocal length. In practice one has to point out some fiducial sphere as the unit sphere to fix the curvedness scale. Curvedness index scale is shown in Figure 2.

The curvedness has some obvious properties that makes it a desirable curvature measure in an intuitive sense [22]:

- the curvedness vanishes only at the planar points. Both the Gaussian and Mean Curvature also vanish at the planar points. The Gaussian Curvature vanishes also on the parabolic curves, however, whereas the Mean Curvature also vanishes on the loci where the surface is locally minimal (that is, $k_1 = -k_2$). But both at the parabolic points, and at the minimal points, the surface has a decidedly "curved look" to most observers;
- the curvedness scales inversely with size;
- the curvedness is trivially coordinate independent, i.e. it has true geometrical significance.

Few authors used shape and curvedness indexes for recognition. Worthington *et al.* [35] investigated whether regions of uniform surface topography can be extracted from intensity images using shape-from-shading and subsequently used for the purposes of thirty object recognition. They draw on the constant Shape Index maximal patch representation of Dorai *et al.*. They showed that the resulting Shape Index regions are stable under different viewing angles. Song *et al.* [31] described a 3D face recognition method using facial Shape Indexes. Given an unknown range image, they extract invariant facial features based on the facial geometry. For face recognition method, they define and extract facial Shape Indexes based on facial curvature characteristics and perform dynamic programming. Shin *et al.* [29] described a pose invariant three-dimensional face recognition method using distinctive facial features. They extract invariant facial feature points on those components using the facial geometry from a normalized face data and calculate relative features using these feature points. They also calculate a Shape Index on each area of facial feature point to represent curvature characteristics of facial components.

3. Parameters benchmarking

To perform the study on facial geometric features, many human faces in person were scanned and used to numerically test the descriptors just introduced. The scanner was a Minolta Vivid 910. Thirty scans of six subjects with different expressions were taken. They are useful to check if the descriptor is strongly connected to the expression or if it is stable between different persons and poses. Real surfaces were never used, but only points that describe the surface shape. These point clouds are called shells. The shells were elaborated by RapidForm, a standard software for 3D scanners. Only the points of the face were kept: the unnecessary, such as hair, ear, neck, parts of collar and clothes, was excluded. A noise filter was applied and little holes were filled. Then the point clouds were triangulated and the mesh was converted into a square grid. The processing and the numerical implementations were performed with Matlab. An example is shown in Figure 1.
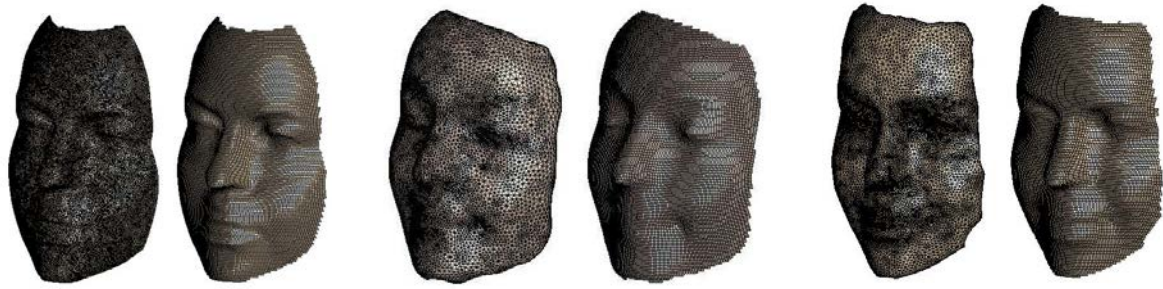
Figure 1. The triangular mesh and the square grid of three scanned faces.

Now a graphical representation of the behaviour of the various descriptors on facial surfaces, one at a time, is here presented. An analysis of each of them is here provided. The goal is to find out the features the these descriptors join among all the faces, in order to collect and use them to describe the similarities of faces. Although every visage is unique, all faces are similar. As a matter of fact, the first step of a recognition algorithm is to search the points common to all faces. Then the comparison between the position of these points of different faces is done, in order to authenticate the subject. But the individuation of the common features is an indispensable first stage for the following steps. This work is focused exactly on the formalization of this analogy, through the use of these elements of Differential Geometry. Every descriptor behaviour will be judged using four parameters:

- **similarity** of the descriptor among various faces and different facial expressions: the analogies between the behaviours of the descriptor among different scans will be analysed;
- **sensitivity** to noise: some inaccuracies during the scanning may present, especially where there is an abrupt changing of colours, namely on the mouth, near the eyes, the eyebrows and the hairline. Some descriptors are more affected by the noise. That is because the acquisition device coincides with the measuring instrument;
- **completeness** in the description of the whole visage: some parameters have an interesting behaviour in many zone of the face, while others accurately describe only one area;
- **smoothness** of their trend (size of the neighborhood): it is a measure of how much gradual is the trend of the descriptor on the face; the presence of isolated points with a very different value is a "not smooth" behaviour. For every descriptor and for every point, its neighborhood is taken into consideration: if the surrounding points have a similar value of the descriptor, then the trend is gradual and the descriptor has a smooth behaviour.

In all the following images, generated with Matlab, red colour corresponds to a high value of the descriptor, while blue corresponds to a low value.

3.1 Coefficients of the Fundamental Forms

The forms (1) and (2) were implemented in order to apply the definitions of these coefficients on the shells point by point. The six coefficients presents different behaviours on the face, as can be seen in Figures 2, 3, 4, 5, 6 and 7.
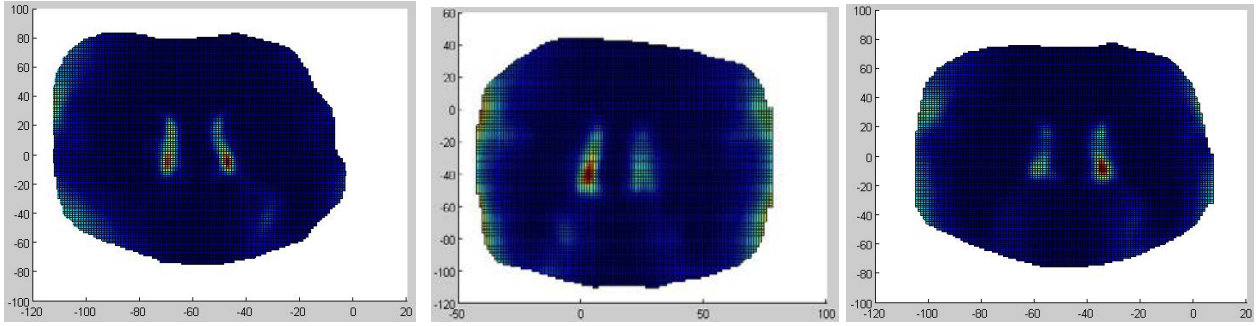
Figure 2. The Coefficient *E* of the First Fundamental Form applied to three facial shells.
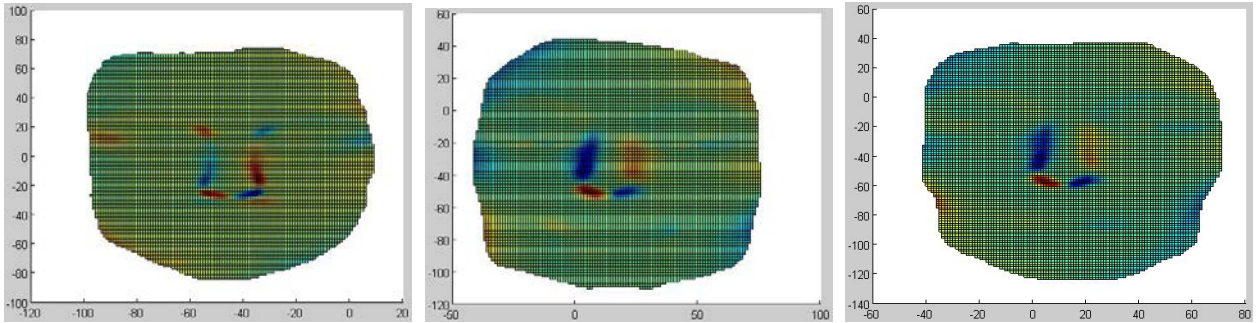

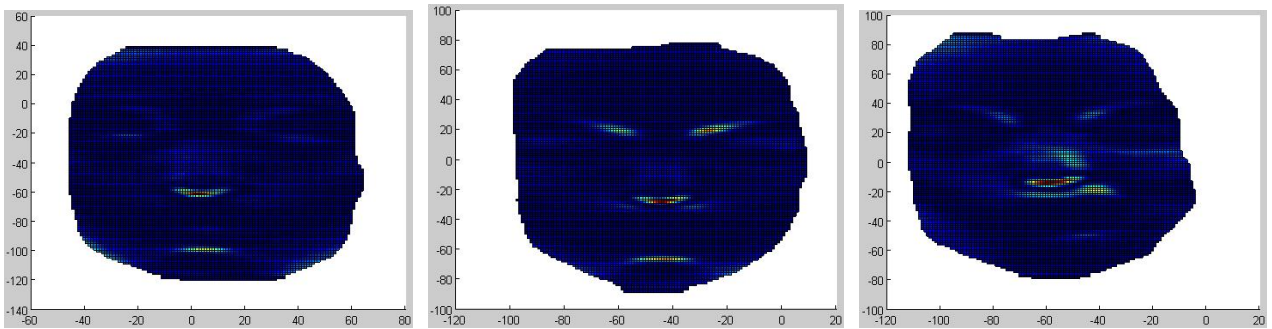**Figure 3. The Coefficient *F* of the First Fundamental Form applied to three facial shells.**

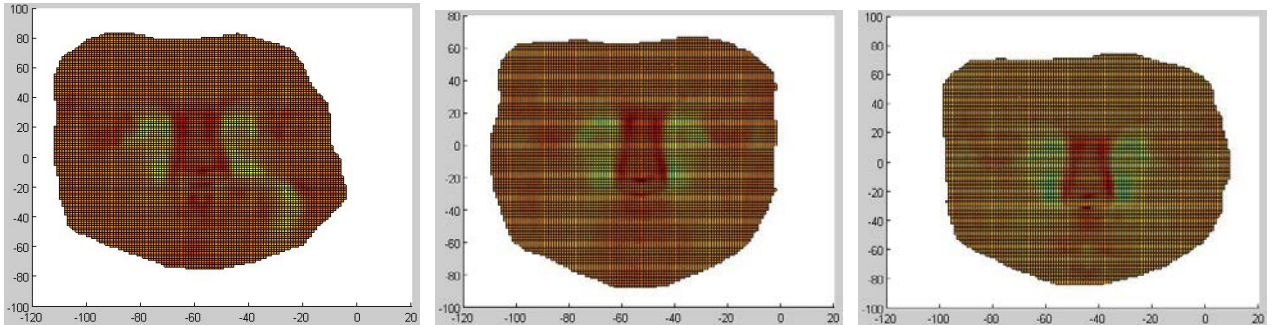**Figure 4. The Coefficient *G* of the First Fundamental Form applied to three facial shells.**

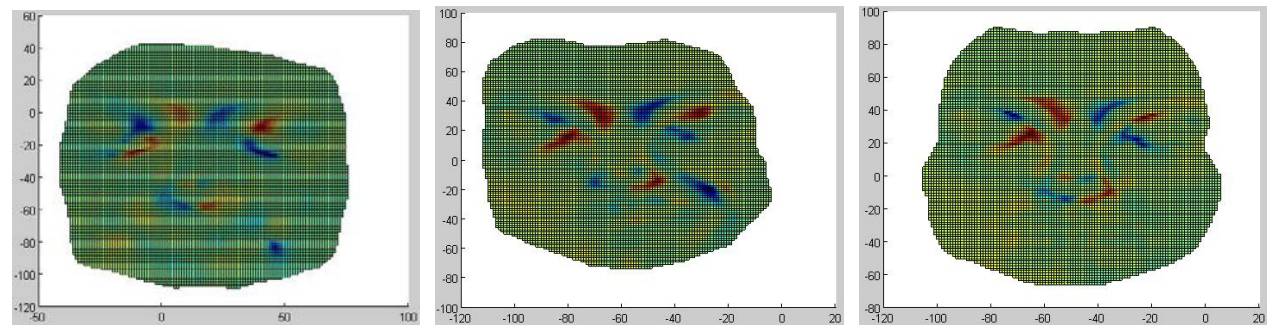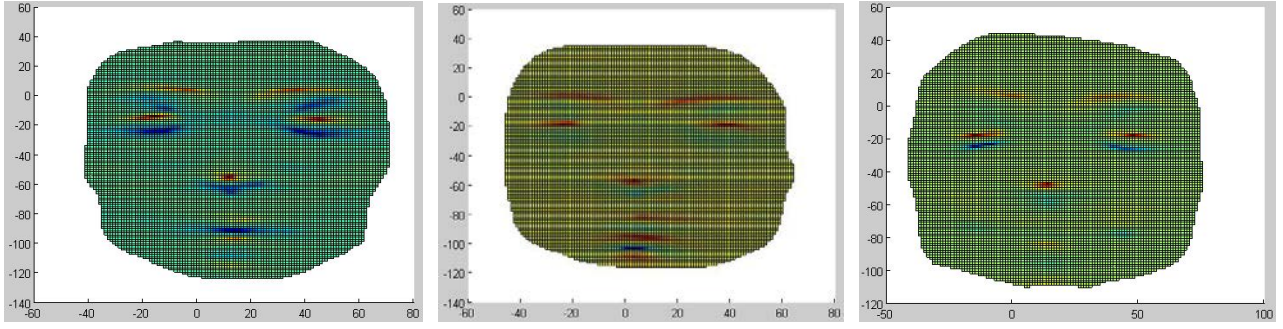**Figure 5. The Coefficient *e* of the Second Fundamental Form applied to three facial shells.**

Figure 6. The Coefficient *f* of the Second Fundamental Form applied to three facial shells.

Figure 7. The Coefficient *g* of the Second Fundamental Form applied to three facial shells.

As can be seen from the images above, the coefficients have similar behaviours in the faces, even though the facial expressions are different. Since the mouth is an area in which the accuracy of the scanning was not as precise as other parts, probably because of the changing in the colour, this zone can be considered, and the areas on the face borders, more sensible to the noise, so less reliable. The same is true for the eyes, that some of the subjects kept close and some kept open during the scanning. Consequently the geometry of these zone may be not so similar for all the shells. From an immediate view can be noticed that only some of these descriptors describe a face in detail: while the graphical representation of *E* and *e* does not give any indication of where mouth and eyes are located, other descriptors, such as *f* and *g*, are more "complete". Probably *g* is the most complete at all: the point of the nose, the little protrusion of the mouth, the eyes and their borders, and even the lines of the eyebrows can be clearly identified. On the contrary, *E* is very restricted to the zones at the two sides of the nose, without giving any description of other parts. All the graphs seem to be quite smooth, namely there are not peaks or points of non-differentiability, such as sharp corners or cusps. Furtheremore, *F* and *f* have an even symmetry with respect to the vertical axis through the centre of the nose, namely what is positive on the left is negative on the right, and viceversa.

3.1 Curvatures

The forms (3) and (4) were implemented to obtain a numerical implementation of the Principal Curvatures, the Gaussian Curvature and the Mean Curvature. Their behaviour on facial surfaces is shown in Figures 8, 9, 10 and 11.
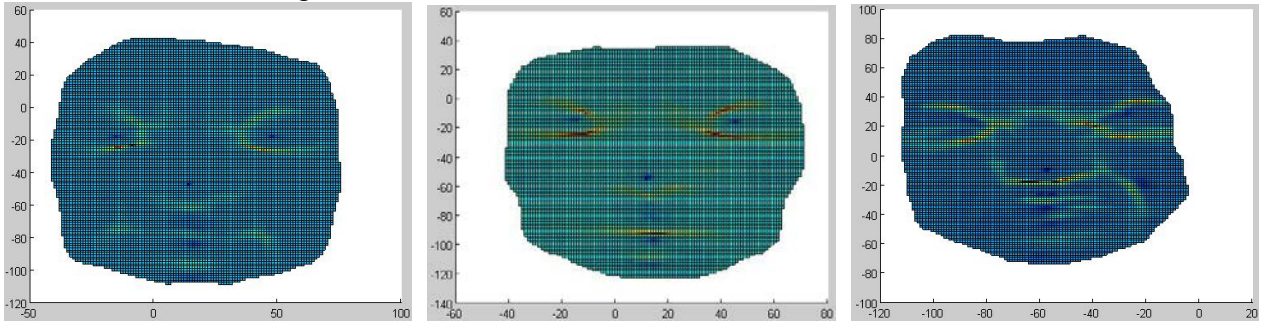

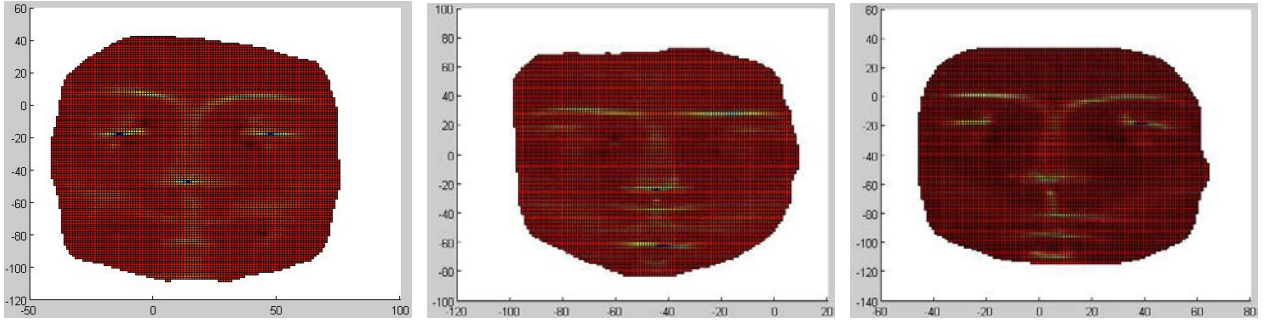**Figure 8. The Principal Curvature k_1 applied to three facial shells.**

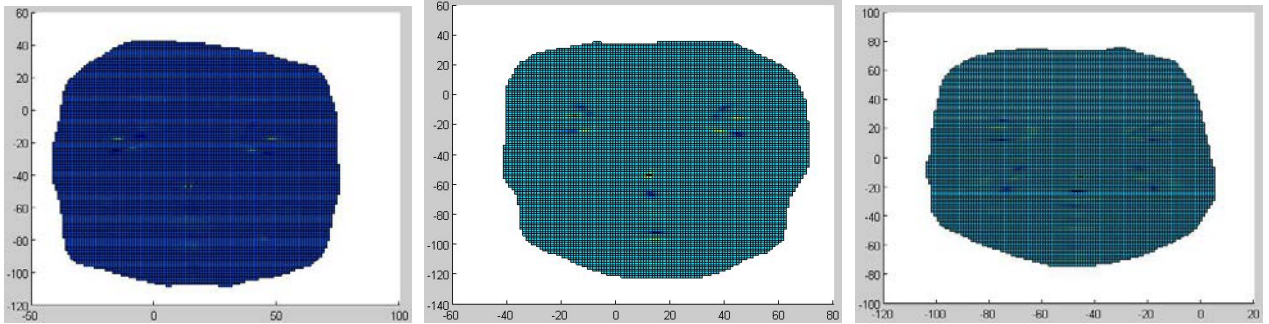**Figure 9. The Principal Curvature k_2 applied to three facial shells.**

Figure 10. The Gaussian Curvature K applied to three facial shells.
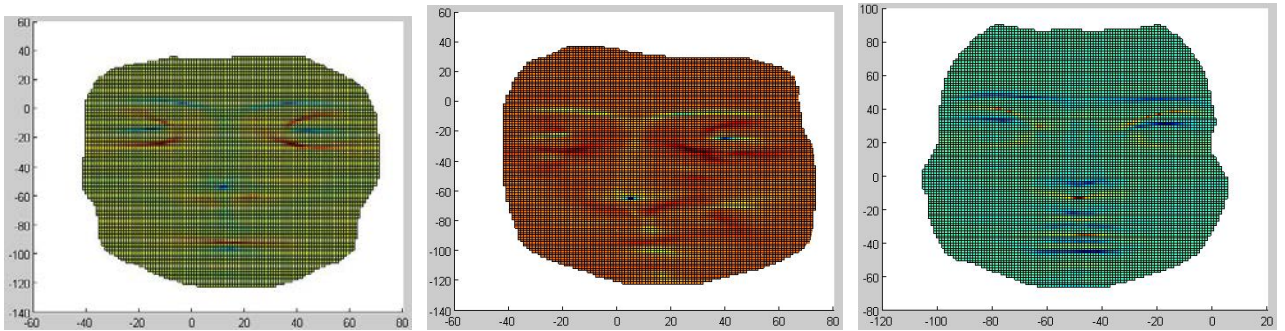

Figure 21. The Mean Curvature H applied to three facial shells.

Although the main colours of the last two images seem to differ among the faces, the behaviour of all these curvatures are similar from face to face. The differences are given by the various facial expressions and by the initial data obtained with the scanning. In fact, the trends are quite analogue. The Principal Curvatures and the Mean Curvature give a complete description of the face, giving the possibility to distinguish the various facial features, even the details around the eyes, while the Gaussian Curvature is the less exhaustive, probably the less complete among the descriptors. Moreover, it is the less smooth, namely its behaviour is made up of peaks and cusps: the maximums and minimums are pointwise and not gradual. This is not true for the other curvatures.

3.3 Derivatives

The derivatives were computed with the function `gradient` of Matlab. For every point of the point cloud it checks the coordinates of the adjacent points and computes the derivative in that point. Axis *x* is vertical, axis *y* is horizontal, axis *z* enters the sheet. In Figures 12, 13, 14, 15 and 16 some behaviours are shown.
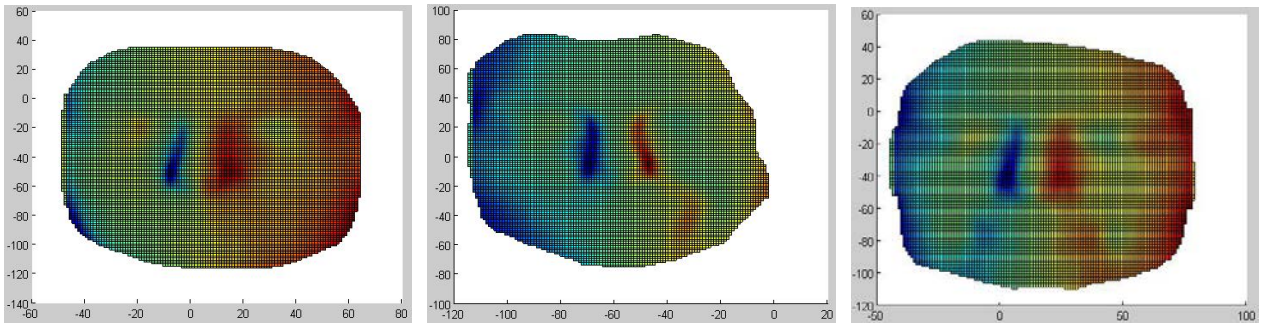
Figure 3. The derivative of *z* with respect to *x*-direction applied to three facial shells.
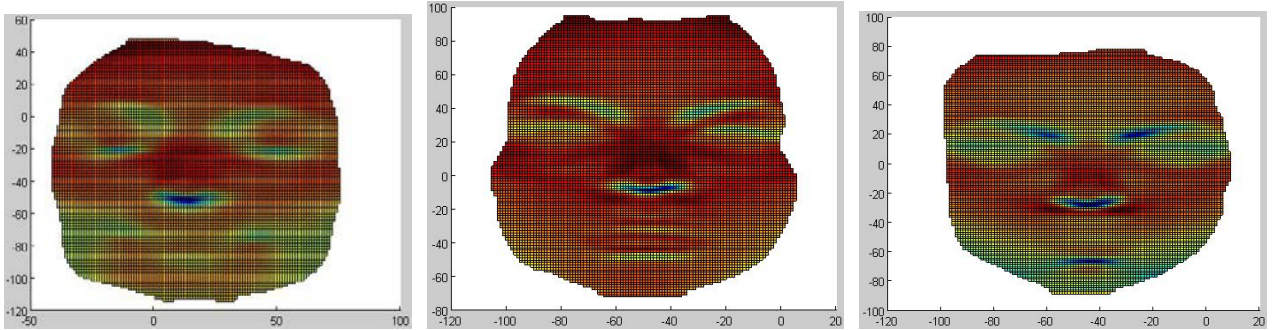

Figure 4. The derivative of *z* with respect to *y*-direction applied to three facial shells.
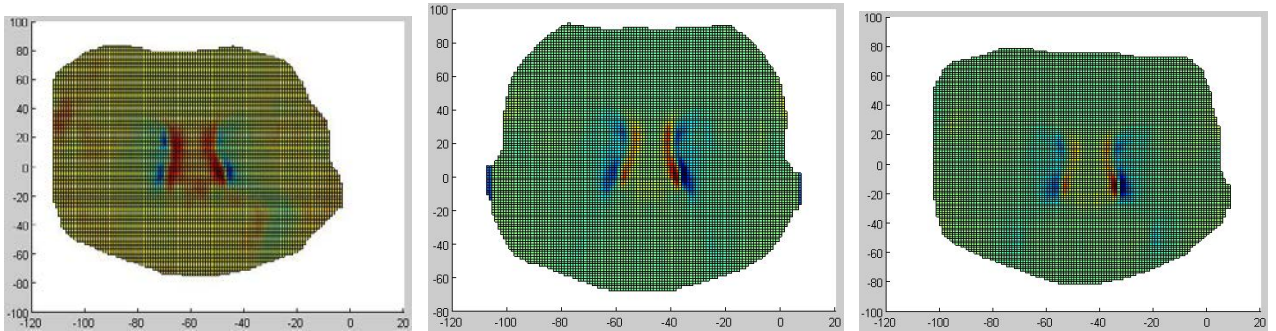

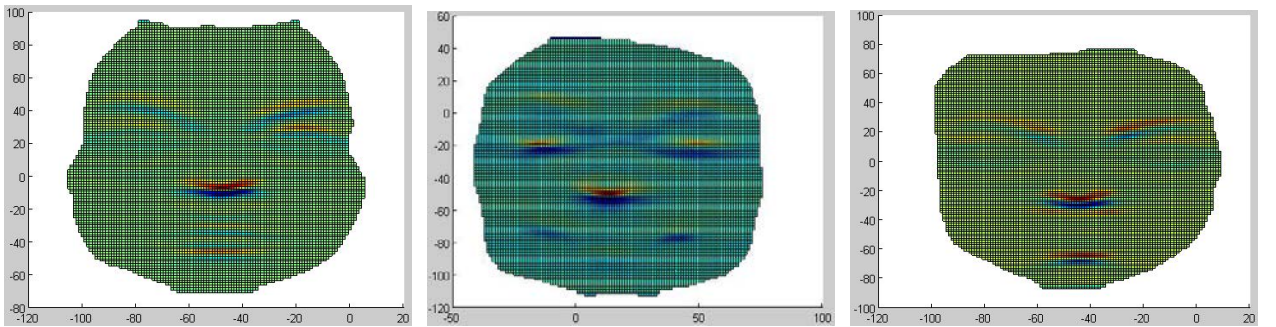**Figure 5. The second derivative of *z* with respect to *x*-direction applied to three facial shells.**

Figure 6. The second derivative of *z* with respect to *y*-direction applied to three facial shells.
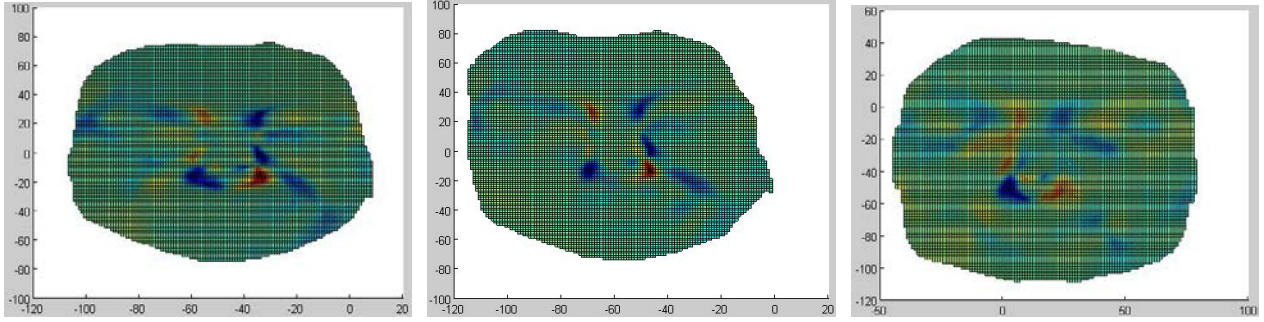
Figure 16. The mixed derivative of *z* applied to three facial shells.

The behaviours of the derivatives among different faces is quite similar, especially for the second derivatives and the mixed the derivative. The first derivatives and the second derivative with respect to *y* give exhaustive information of many parts of the face, above all the first derivative with respect to *y*. Contrariwise the second derivative of z with respect to x gives only partial information, only in the area of the nose. Moreover, the first derivatives are very smooth, probably the smoothest of this study: the increments and decreases are gradual.

3.4 Shape and Curvedness Indexes

Forms (5) and (6) were used to numerically implement the forms for *S* and C. The images shown if Figures 17 and 18 were obtained.
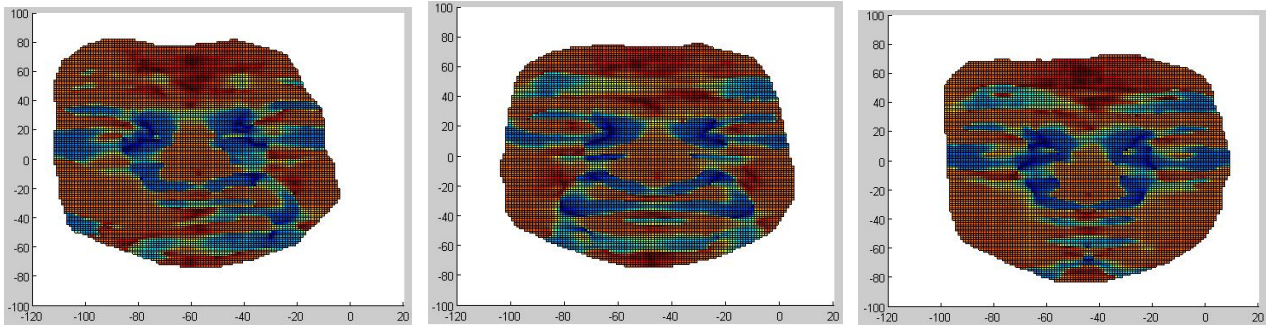

Figure 17. The behaviour of the Shape Index applied to three facial shells. Red points are the ones corresponding to a high value of the index (dome surface), while blue ones correspond to a low value (cup surface).
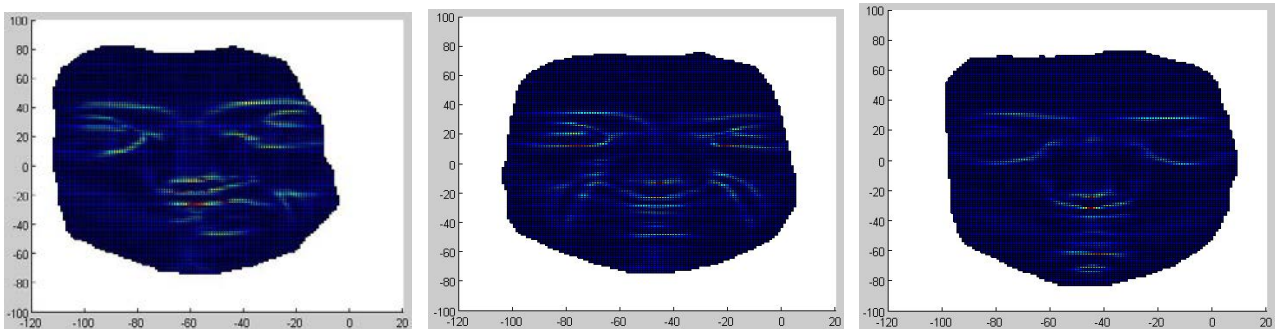

Figure 18. The behaviour of the Curvedness Index applied to the same three shells. The wrinkles near the mouth and the nose of the first and the second shells can be noticed: they are consequences of the crimped expression of the face. The red points have a higher value of the index.

The behaviour of the Indexes are similar among the two faces, although the facial expression differs. Generally, cheeks, lips, bottom nose, pupils and forehead have a high value of S, while the inner corners of eyes and the zone around the nose have low values of the Shape Index. Saddle points, such as the part on the top of the nose and the little hollow between nose and mouth, have medium values, close to zero. The lighter zones of the Curvedness Index correspond to those areas in which the curvature brusquely change value: eyebrows, eyelids, nose and lips. The areas close to the mouth may be considered more sensitive to the nose and so less reliable. These descriptor are

very complete: by their definition and the structure of the face, they are able to describe accurately every part of the face, even focusing the zones, such as the saddle points, less easily identifiable. They are not very smooth, but for their role in the description, it does not matter at all.

4. Discussion and conclusion

The descriptors are judged and classified according to the four parameters. A good mark (1 is bad, 10 is excellent) in similarity means that the descriptor has a similar behaviour in all the shells; a good mark in sensitivity means that it is not sensitive to the noise, namely the descriptor does not focus its description on the zones more affected by the noise, i.e. mouth and eyelids; a good mark in completeness implies that the descriptors well portrays many areas of the face; a good mark in smoothness means that its behaviour is smooth: its trend is gradual. The marks are shown in Table 1 and in the graphical representation of Figure 19.

The evaluation is performed thanks to the graphs and the images here reported previously. The behaviour of the descriptors allow a precise examination of their trends, based on the parameters chosen for the judgement.

	similarity	sensitivity	completeness	smoothness
E	10	10	6	8
F	9	10	7	8
G	7	8	7	8
e	8	10	7	8
f	9	10	7	8
g	8	8	9	8
k_1	8	7	8	7
k_2	8	7	8	7
K	8	7	6	6
H	8	7	9	7
D_x	10	10	7	10
D_y	7	7	9	10
D_{xx}	10	10	6	8
D_{yy}	7	7	8	8
D_{xy}	8	9	8	8
S	7	7	10	6
C	7	7	10	6

Table 1. The descriptors are judged according to the parameters.
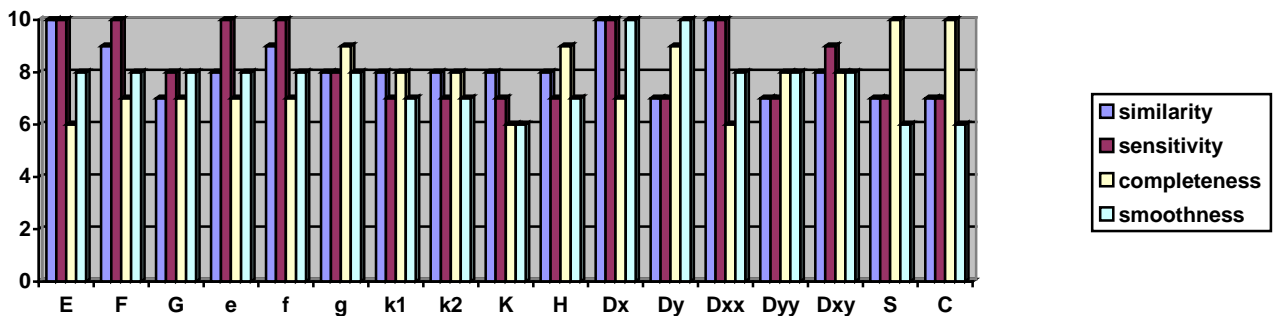

Figure 19. Marks of the descriptors referred to the parameters.

The descriptors show good marks for every parameter. This means that these descriptors are not only valid, but even suitable for a face description. Averaging the marks for every descriptor a diagram of the results was done, in order to have a graphical view of their usefulness. It is reported in Figure 20.
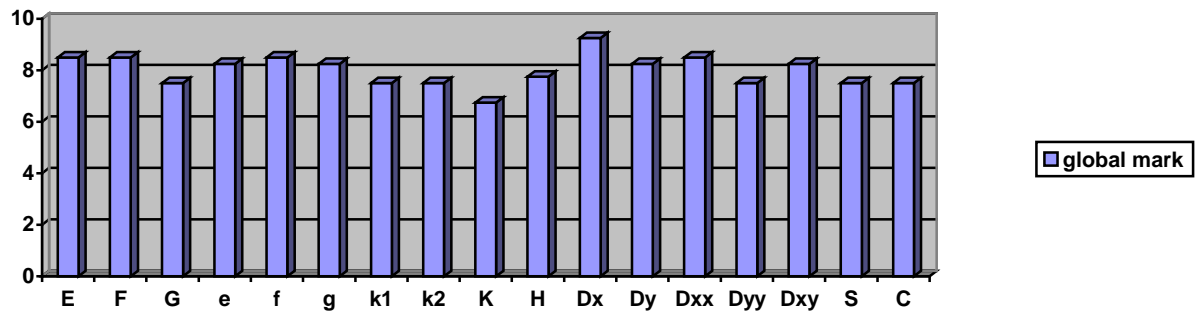

Figure 20. Global marks of the descriptors, obtained with an average.

The global marks are quite good for all the descriptors. The best evaluation is given to the derivative with respect to *x*, whose behaviour is very similar among different faces and facial expressions, is not very sensitive to noise and is the smoothest between the geometrical elements. The worst is the Gaussian Curvature. It is not complete and not very smooth: many punctual values are present in its trend.

The attention was here focused to some descriptors of Differential Geometry applied to the human face, giving a survey of their behaviours on facial surface. They were classified according to four parameters, whose meaning may be easily and concretely checked. This is a starting point for a complete geometrical description of faces. In the next work, landmarks will be used, namely some scientific points of reference on the face, which all faces join and with a particular biological meaning. It will be shown how to use these descriptors as a means for recognition, identifying the areas of interest which the landmarks lies in and then extracting them accurately. The goal is most of all to show how recognition is possible only using geometry.

6. References

[1] ALYUZ, N., DIBEKLIOGLU, H., GOKBERK, B. AND AKARUN, L. (2008) "Part-based registration for expression resistant 3D face recognition", *IEEE 16th Signal Processing, Communication and Applications Conference*, 1-4.

[2] AMBERG, B., KNOTHE, R. AND VETTER, T. (2008) "Expression invariant 3D face recognition with a Morphable Model", *8th IEEE International Conference on Automatic Face and Gesture Recognition*, 1-6.

[3] AMOR, B. B., ARDABILIAN, M. AND LIMING, C. (2006) "New Experiments on ICP-Based 3D Face Recognition and Authentication", *18th International Conference on Pattern Recognition*, 1195-1199.

[4] CADAVID, S., ZHOU, J. AND ABDEL-MOTTALEB, M. (2009) "Determining discriminative anatomical point pairings using AdaBoost for 3D face recognition", *16th IEEE International Conference on Image Processing (ICIP)*, 49-52.

[5] CALIGNANO, F. (2009) *Morphometric methodologies for bio-engineering applications*, PhD Degree Thesis, Politecnico di Torino, Department of Production Systems and Business Economics.

[6] D'HOSE, J., COLINEAU, J., BICHON, C. AND DORIZZI, B. (2007) "Precise Localization of Landmarks on 3D Faces using Gabor Wavelets", *First IEEE International Conference on Biometrics: Theory, Applications, and Systems*, 1-6.

[7] DO CARMO, M., *Differential Geometry of Curves and Surfaces*, Prentice-Hall Inc., Englewood Cliffs, New Jersey, 1976.

[8] DORAI, C. AND JAIN, A. K. (1997) "COSMOS - A Representation Scheme for 3D Free-Form Objects", *IEEE Transactions on Pattern Analysis and Machine Intelligence*, 19(10): 1115-1130.

[9] ELAD, A. AND KIMMEL, R. (2001) "Bending invariant representations for surfaces", *IEEE Computer Society Conference on Computer Vision and Pattern Recognition*, 1: I-168 - I-174.

[10] ELAD, A. AND KIMMEL, R. (2003) "On bending invariant signatures for surfaces", *IEEE Transactions on Pattern Analysis and Machine Intelligence*, 25(10): 1285 – 1295.

[11] ELYAN, E. AND UGAIL, H. (2009) "Automatic 3D Face Recognition Using Fourier Descriptors", *International Conference on CyberWorlds - IEEE Conferences*, 246-252.

[12] ESSANNOUNI, L., ELHAJ, E. I. AND ABOUTAJDINE, D. (2007) "Automatic face tracking and identity verification", 14th IEEE International Conference on Electronics, Circuits and Systems, 335-338.

[13] FABRY, T., VANDERMEULEN, D. AND SUETENS, P. (2008) "3D Face Recognition using Point Cloud Kernel Correlation", *2nd IEEE International Conference on Biometrics: Theory, Applications and Systems*, 1-6.

[14] GOLDGOF, D. B. AND MISHRA, S. K. (1991) "Motion analysis and modeling of epicardial surfaces from point and line correspondences", *Proceedings of the IEEE Workshop on Visual Motion*, 300-305.

[15] GOLDGOF, D. B., MISHRA, S. K. AND KAMBHAMETTU, C. (1994) "Estimating non-rigid motion from point and line correspondences", *Pattern Recognition Letters*, ScienceDirect, 15(6): 559-566.

[16] GOLDGOF, D. B., KAMBHAMETTU, C., HE, P. AND LASKOV, P. (2003) "3D nonrigid motion analysis under small deformations", *Image and Vision Computing*, ScienceDirect, 21(3): 229-245.

[17] GRAY, A., ABBENA, E. AND SALAMON, S., *Modern Differential Geometry of Curves and Surfaces with Mathematica*, CRC Press, Boca Raton, Florida, 2006.

[18] GUNLU, G. AND BILGE, H. S. (2009) "3D transformation based feature extraction and selection for 3D face recognition", *IEEE 17th Signal Processing and Communications Applications Conference*, 436-439.

[19] GUNLU, G. AND BILGE, H. S. (2009) "Feature extraction and discriminating feature selection for 3D face recognition", *24th International Symposium on Computer and Information Sciences*, 44-49.

[20] HARGUESS, J., GUPTA, S. AND AGGARWAL, J. K. (2008) "3D face recognition with the average-half-face", *19th International Conference on Pattern Recognition - IEEE Conferences*, 1-4.

[21] JINYE, P. AND YU, B. (2001) "Multi-scale Bayesian face recognition by using anti-symmetrical biorthogonal wavelets", *International Conferences on Info-tech and Info-net*, 3: 414-420.

[22] KOENDERINK, J. J. AND VAN DOORN, A. J. (1992) "Surface shape and curvature scales", *Image and Vision Computing*, 10(8): 557-564.

[23] LEI, Y., CHEN, D., YUAN, M., LI, Q. AND SHI, Z. (2009) "3D Face Recognition by Surface Classification Image and PCA", *Second International Conference on Machine Vision - IEEE Conferences*, 145-149.

[24] MAHOOR, M. H. AND ABDEL-MOTTALEB, M. (2007) "3D Face Recognition Based on 3D Ridge Lines in Range Data", *IEEE International Conference on Image Processing*, I: 137-140.

[25] MIAN, A. S. (2009) "Shade Face: Multiple image-based 3D face recognition", *IEEE 12th International Conference on Computer Vision Workshops (ICCV Workshops)*, 1833-1839.

[26] MING, Y. AND RUAN, Q. (2010) "Orthogonal Laplacianfaces for 3D face recognition", *2nd International Conference on Industrial and Information Systems (IIS) - IEEE Conferences*, 277 - 280.

[27] QUEIROLO, C. C., SILVA, L., BELLON, O. R. P. AND SEGUNDO, M. P. (2010) "3D Face Recognition Using Simulated Annealing and the Surface Interpenetration Measure", *IEEE Transactions on Pattern Analysis and Machine Intelligence*, 206-219.

[28] QUEIROLO, C. C., SILVA, L., BELLON, O. R. P. AND SEGUNDO, M. P. (2007) "Noise versus Facial Expression on 3D Face Recognition", *14th International Conference on Image Analysis and Processing – IEEE Conferences*, 171-178.

[29] SHIN, H. AND SOHN, K. (2006) "3D Face Recognition with Geometrically Localized Surface Shape Indexes", *9th International Conference on Control, Automation, Robotics and Vision - IEEE Conferences*, 1-6.

[30] SMEETS, D., FABRY, T., HERMANS, J., VANDERMEULEN, D. AND SUETENS, P. (2010) "Fusion of an Isometric Deformation Modeling Approach Using Spectral Decomposition and a Region-Based Approach Using ICP for Expression-Invariant 3D Face Recognition", *20th International Conference on Pattern Recognition (ICPR)*, 1172-1175.

[31] SONG, H., YANG, U., LEE, S. AND SOHN, K. (2005) "3D Face Recognition Based on Facial Shape Indexes with Dynamic Programming", *Lecture Notes in Computer Science*, Springer-Verlag, 3832: 99-105.

[32] SUN, Y. AND YIN, L. (2005) "3D Face Recognition Using Two Views Face Modeling and Labeling", *IEEE Computer Society Conference on Computer Vision and Pattern Recognition*, 117-117.

[33] VEZZETTI, E. AND CALIGNANO, F. (2010) "A Morphological Methodology for Three-dimensional Human Face Soft-tissue Landmarks Extraction: A Preliminary Study", *Aesthetic Plastic Surgery*, DOI 10.1007/s00266-010-9579-6, Springer.

[34] VEZZETTI, E. AND MOSCHINI, P., (????) *Study and Development of Morphological Analysis Guidelines for Point Cloud Management: the "Decisional Cube"*, Politecnico di Torino, Department of Production Systems and Business Economics.

[35] WORTHINGTON, P. L. AND HANCOCK, E. R. (2000) "Structural Object Recognition using Shape-from-Shading", *15th International Conference on Pattern Recognition - IEEE Conferences*, Vol.1: 738-741.

[36] XIAOGUANG, L. AND JAIN, A. K. (2005) "Integrating Range and Texture Information for 3D Face Recognition", *7th IEEE Workshops on Application of Computer Vision*, Vol.1: 156-163.

[37] YI, S. AND LIJUN, Y. (2008) "3D Spatio-Temporal face recognition using dynamic range model sequences", *IEEE Computer Society Conference on Computer Vision and Pattern Recognition Workshops*, 1-7.

[38] YONG-AN, L., YONG-JUN, S., GUI-DONG, Z., TAOHONG, Y., XIU- JI, X. AND HUA-LONG, X. (2010) "An Efficient 3D Face Recognition Method Using Geometric Features", *2nd International Workshop on Intelligent Systems and Applications (ISA) - IEEE Conferences*, 1-4.

[39] YONGSHENG, G., BAOCHANG, Z., SANQIANG, Z. AND JIANZHUANG, L. (2010) "Local Derivative Pattern Versus Local Binary Pattern: Face Recognition With High-Order Local Pattern Descriptor", *IEEE Transactions on Image Processing*, 2246-2249.

[40] YONGSHENG, Z., SANQIANG, Z. AND CAELLI, T. (2010) "High-Order Circular Derivative Pattern for Image Representation and Recognition", *20th International Conference on Pattern Recognition (ICPR)*, 19(2): 533-544.

[41] Face Recognition Homepage
http://www.face-rec.org/algorithms